



CONTRIBUTION TO MODELLING OF CONTACT BETWEEN WHEEL SET AND CURVED RAILWAY

J. Švígler*, J. Siegl*

Summary: *The contribution deals with the modelling of the rolling contact between the wheel set of the railway vehicle and the curved railway and subsequently with the lateral motion of the wheel set on this railway. The motion is separate into kinematic motion and dynamic motion. Results of the numerical solution of both motions are compared with results of the wheel set motion on the straight railway which was solved in submission at this conference in the last year.*

1. Introduction

The preliminary analysis of rolling contact between the wheel of the railway vehicle and rail and origin the forces that develop in the contact patch was solved in work Švígler & Vimmr (2006) where the rise and determination of creep forces was discussed. The solution of rolling contact is based on Kalker's linear theory (Kalker J. J., 1979; Garg V. K. & Dukkipati R. V., 1984) which suggests (De Pater A. D., 1962) that for very small creepages γ_i , $i = 1, 2, 3$ (Švígler & Vimmr, 2006), the area of slip in the contact patch is so small that its influence can be neglected. Then the contact patch can be considered as closed adhesion zone and therefore it is possible the contact between wheel and rail interprets as contact at point. For expression of forces it is considered contact patch which is substituted by area of ellipse. After then the contact simplifies into geometric contact without mutual penetration of both bodies. On this condition can be assumed that the generating force is determined by Hooke's law. Kalker (Kalker J. J., 1979) has shown that the linear creep forces depend on creepages in accordance with relation

$$\mathbf{F}_{creep} = \mathbf{K}\mathbf{g}, \quad (1)$$

where \mathbf{F}_{creep} is vector of creep force effects at contact point, \mathbf{K} is a square matrix of Kalker's linear coefficients and \mathbf{g} is a vector of creepage coefficients. After expressing of this matrices and their substituting into Eq. (1) we obtain

* Doc. Ing. Jaromír Švígler, CSc., Ing. Jaroslav Siegl: University of West Bohemia, Faculty of Applied Sciences, Department of Mechanics; Univerzitní 22; 301 00 Pilsen; e-mail: svigler@kme.zcu.cz, jsiegl@kme.zcu.cz; phone: +420 377 632 304, +420 377 632 381

$$\mathbf{F}_{creep} = \begin{bmatrix} T_x \\ T_y \\ M_z \end{bmatrix} = \begin{bmatrix} (ab)GC_{11} & 0 & 0 \\ 0 & (ab)GC_{22} & (ab)^{\frac{3}{2}}GC_{23} \\ 0 & (ab)^{\frac{3}{2}}GC_{32} & (ab)^2GC_{33} \end{bmatrix} \begin{bmatrix} \gamma_1 \\ \gamma_2 \\ \gamma_3 \end{bmatrix}, \quad C_{23} = C_{32}, \quad (2)$$

where T_x, T_y are longitudinal and lateral creep forces and M_z is spin-creep moment (Švígler & Vimmr, 2006). C_{ij} are creepage and spin coefficients which depend on Poisson's material constant σ of wheel and rail and on the ratio of the semiaxes of the contact ellipse. Semiaxes a and b in longitudinal and lateral direction are depended on radius of curvature of wheel and rail (Švígler & Vimmr, 2006). The coefficients C_{ij} are given in a discrete form (Garg & Dukkipati, 1984) and G is shear modulus of rigidity which depends on shear modulus of rigidity of wheel and rail. The Eq. (1) can be simplified into form

$$\mathbf{F}_{creep} = \begin{bmatrix} T_x \\ T_y \\ M_z \end{bmatrix} = \begin{bmatrix} f_{11} & 0 & 0 \\ 0 & -f_{22} & -f_{23} \\ 0 & f_{23} & -f_{33} \end{bmatrix} \begin{bmatrix} \gamma_1 \\ \gamma_2 \\ \gamma_3 \end{bmatrix}, \quad (3)$$

where f_{ij} are the linear creep coefficients. Creep forces are modified by Johnson and Vermeulen theory (Iwnicki, 2003) for reason of creep force linearization because tangential force size can not overpass value fN . The discrete form of coefficients C_{ij} and auxiliary coefficients m_a, m_b for determination of semiaxes a, b of contact ellipse were approximated (Siegl & Švígler, 2006) by spline functions, Fig. 1.

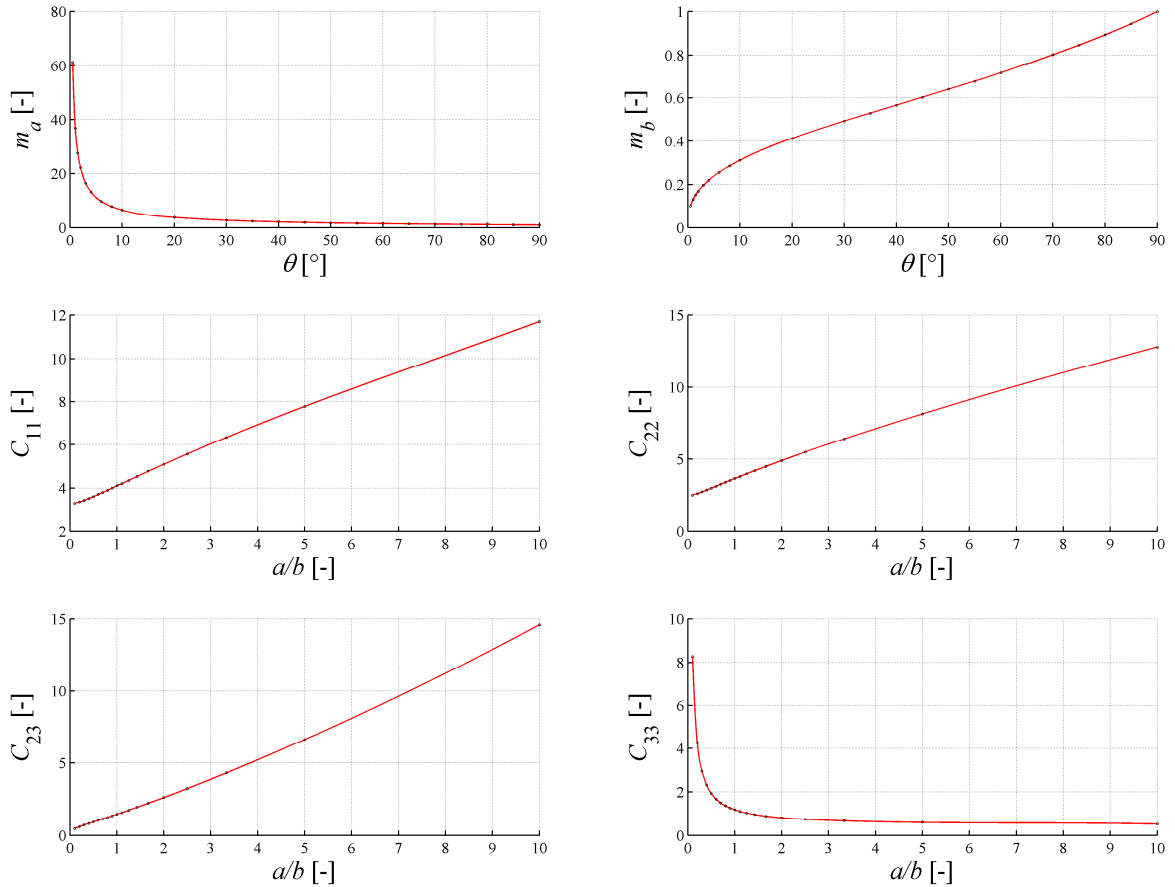


Fig. 1 Continuous functions m_a, m_b, C_{ij} (redly) and discrete values (black points)

2. Simulation of kinematic wheel set motion on curved railway

For the simulation of kinematic wheel set lateral motion on curved railway, Fig 2, the results of moving of the same one in straight railway which was obtained formerly (Švígler & Vimmr, 2006) can be used.

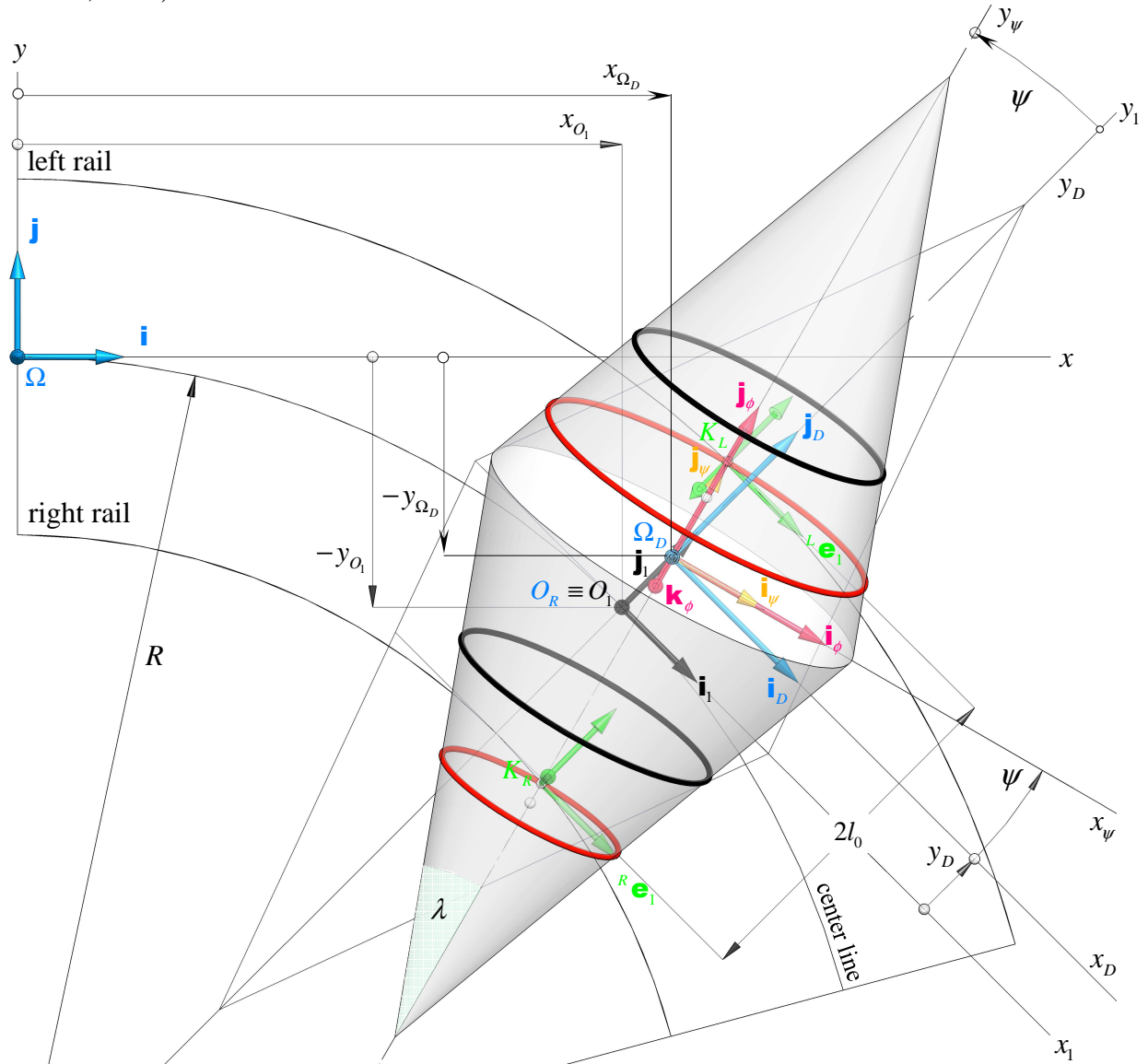


Fig. 2 Free wheel set motion on the curved railway

It is only necessary put into moving equations for the straight railway instead of the deviation y its extended, Fig. 2, relation

$$-y \equiv -y_{\Omega_D} \approx -y_{O_1} + y_D. \quad (4)$$

After then it is possible for the radius of curvature of railway central line to write expression

$$\frac{d^2 y_{\Omega_D}}{dx_{\Omega_D}^2} = \frac{1}{\rho} = \frac{\tan \lambda}{r_w l_0} y_D = \frac{\tan \lambda}{r_w l_0} (y_{O_1} - y_{\Omega_D}), \quad (5)$$

where y_{Ω_D} and x_{Ω_D} are, Fig. 2, coordinates of wheel set center, y_{O_1} is coordinate of origin O_1 of the coordinate system $R_1 \equiv (\mathbf{i}_1, \mathbf{j}_1, \mathbf{k}_1)$ which lies on railway central line, r_w is the teoretical

rolling radius and y_D in Eq. (4) determines wheel set lateral moving. Because $R \gg y_D$ it is assumed that coordinate of wheel set centre Ω_D , with respect to origin O_1 , in direction of axis y is approximately the same, Fig. 2, as lateral moving y_D .

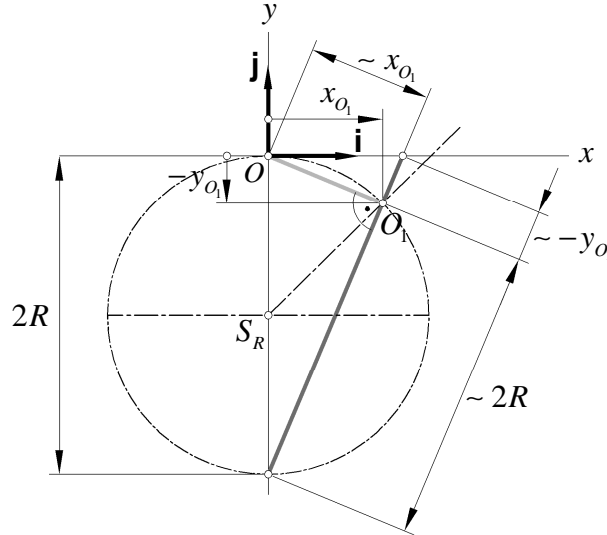


Fig. 3 Determination of coordinates

Using of Euclid's theorem (Švejnoch a kolektiv, 1991) we can, Fig. 3, near the origin Ω of space $R \equiv (\mathbf{i}, \mathbf{j}, \mathbf{k})$, obtain, with plausible approximation, relation between y_{O_1} and x_{O_1}

$$y_{O_1} \doteq -\frac{x_{O_1}^2}{2R}. \quad (6)$$

After inserting into Eq. (5) and with the substitution $x_{\Omega_D} = x$, $y_{\Omega_D} = y$, for better lucidity for next solution, we get

$$\frac{d^2 y}{dx^2} + y\Omega^2 = -\frac{x_{O_1}^2}{2R}\Omega^2, \quad (7)$$

where $\Omega^2 = \frac{\text{tg } \lambda}{r_w l_0}$ is length frequency. Complete solution of Eq. (7), that determines lateral motion of wheel set in space R, Fig. 4, is

$$y = \left(y_0 - \frac{1}{R\Omega^2} \right) \cos \Omega x + \frac{y'_0}{\Omega} \sin \Omega x + \frac{1}{R} \left(\frac{1}{\Omega^2} - \frac{x^2}{2} \right), \quad (8)$$

where $y_0 = y(0)$, $y'_0 = y'(0)$ are initial conditions. It is evident to see that frequency of oscillating motion is the same as for the straight railway and the amplitude depends on the curvature radius R of railway central line.

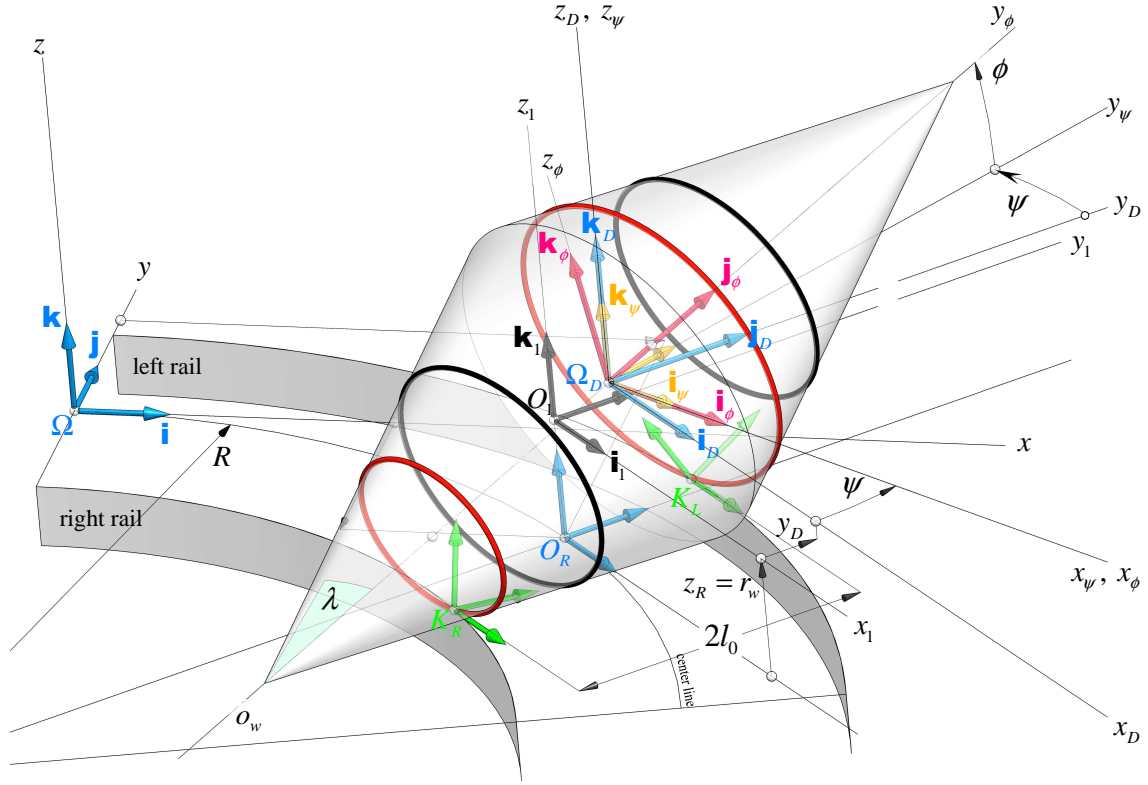


Fig. 4 Space arrangement of coordinate spaces

The particular solution of Eq. (8) expresses static displacement of the wheel set on arc so that the wheel set, according with Eq. (8), oscillates in lateral direction around the equidistant line to the railway central line, distance Δ , that is dislocated face out from arc. Lateral motion in space R_1 is given with relation

$$y_D = y_{O_1} - y = -(y_0 - \Delta) \cos \Omega x - \frac{y'_0}{\Omega} \sin \Omega x - \Delta + \frac{x^2}{2R} - \frac{x_{O_1}^2}{2R}, \quad (9)$$

where $\Delta = \frac{1}{R\Omega^2}$ and $x = vt$, v is velocity of forward movement of wheel set centre Ω_D . The lateral motion was considered as motion with one degree of freedom, i.e. the swaying motion around axis x_D was not accepted. Rotary motion ψ around axis z_D can be expressed by time differentiation of $y = x(t)$ because

$$\psi = \arctg \frac{dy}{dx} = \arctg \left[\left(\frac{1}{R\Omega} - y_0 \Omega \right) \sin \Omega x + y'_0 \cos \Omega x - \frac{x}{R} \right]. \quad (10)$$

Then we obtain

$$\dot{\psi} = \frac{v}{1 + \left[\left(\frac{1}{R\Omega} - y_0 \Omega \right) \sin \Omega x + y'_0 \cos \Omega x - \frac{x}{R} \right]^2} \left[\left(\frac{1}{R} - y_0 \Omega^2 \right) \cos \Omega x - y'_0 \Omega \sin \Omega x - \frac{1}{R} \right]. \quad (11)$$

The comparison of wheel set lateral oscillation on the straight and curved, $R = 500$ m, railway for the same entry conditions is demonstrated in Fig. 5.

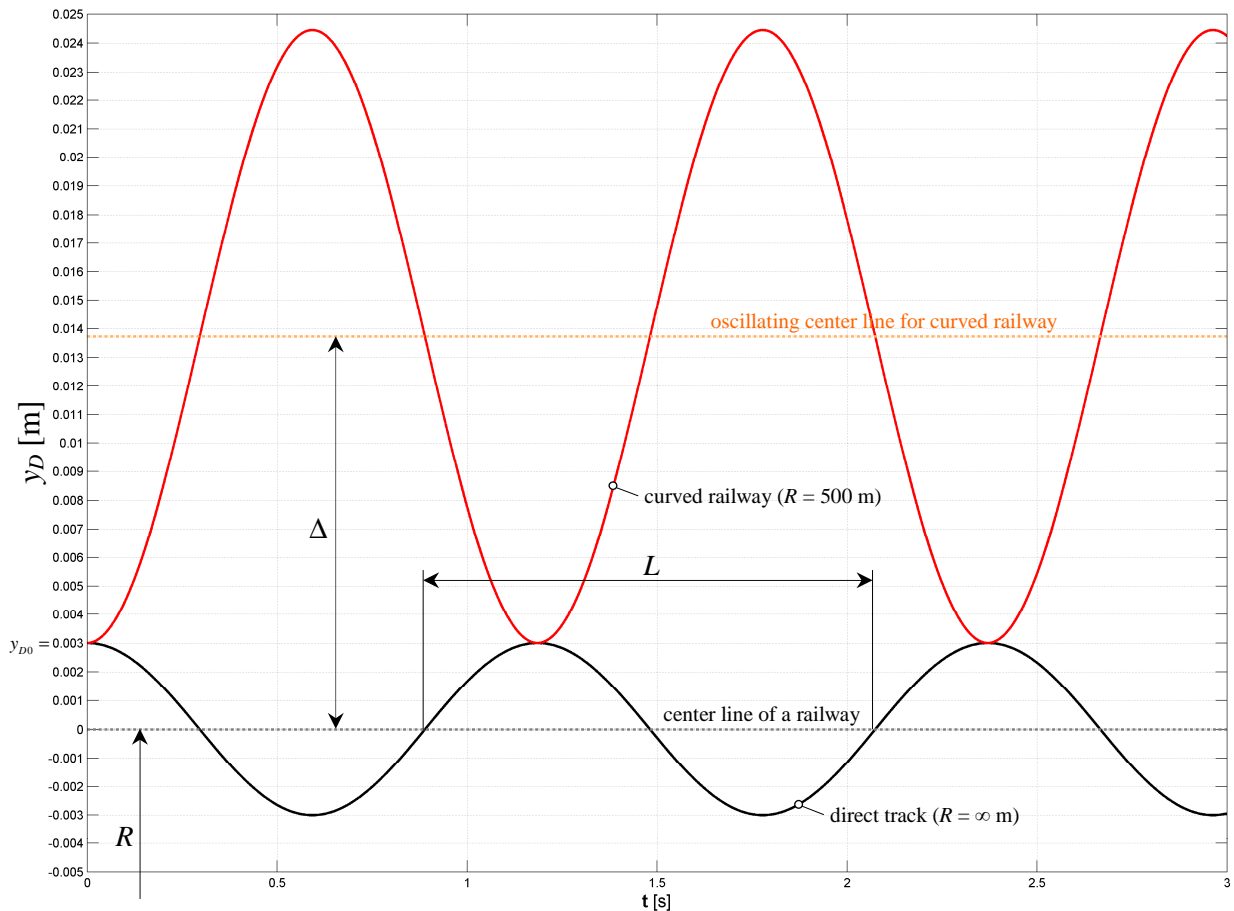


Fig. 5 Comparison of wheel set oscillation on direct and curved railway for $R = 500$ m, $v = 50$ km/h, $y_{D0} = 0,003$ m

The lateral oscillation of wheel set on the curved railway, depending on radius of the railway arc, is shown in Fig. 6. Fig. 7 demonstrates influence of initial quantity of the lateral displacement y_{D0} on the vibration amplitude y .

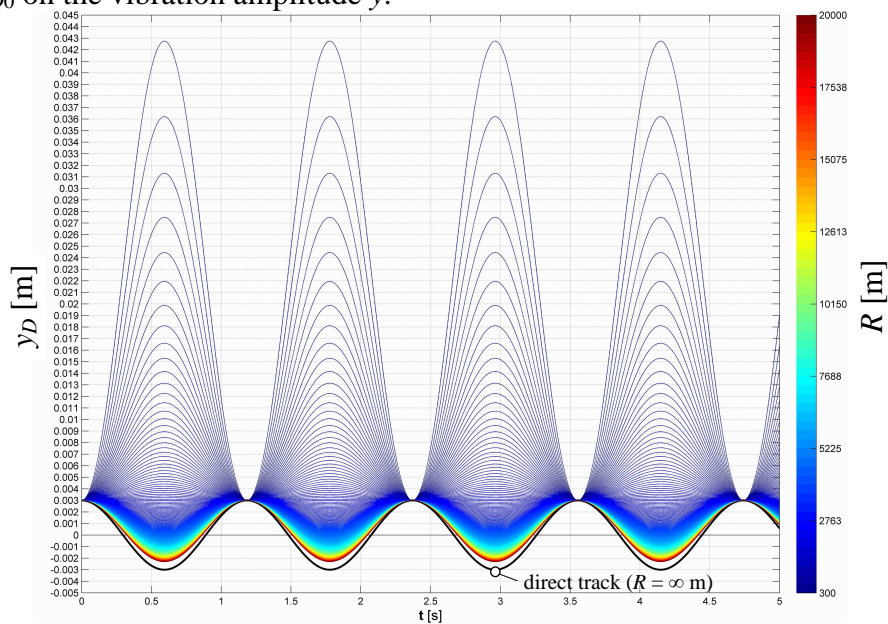


Fig. 6 Lateral motion on curved railway depending on time t and radius R for $y_{D0} = 0,003$ [m]

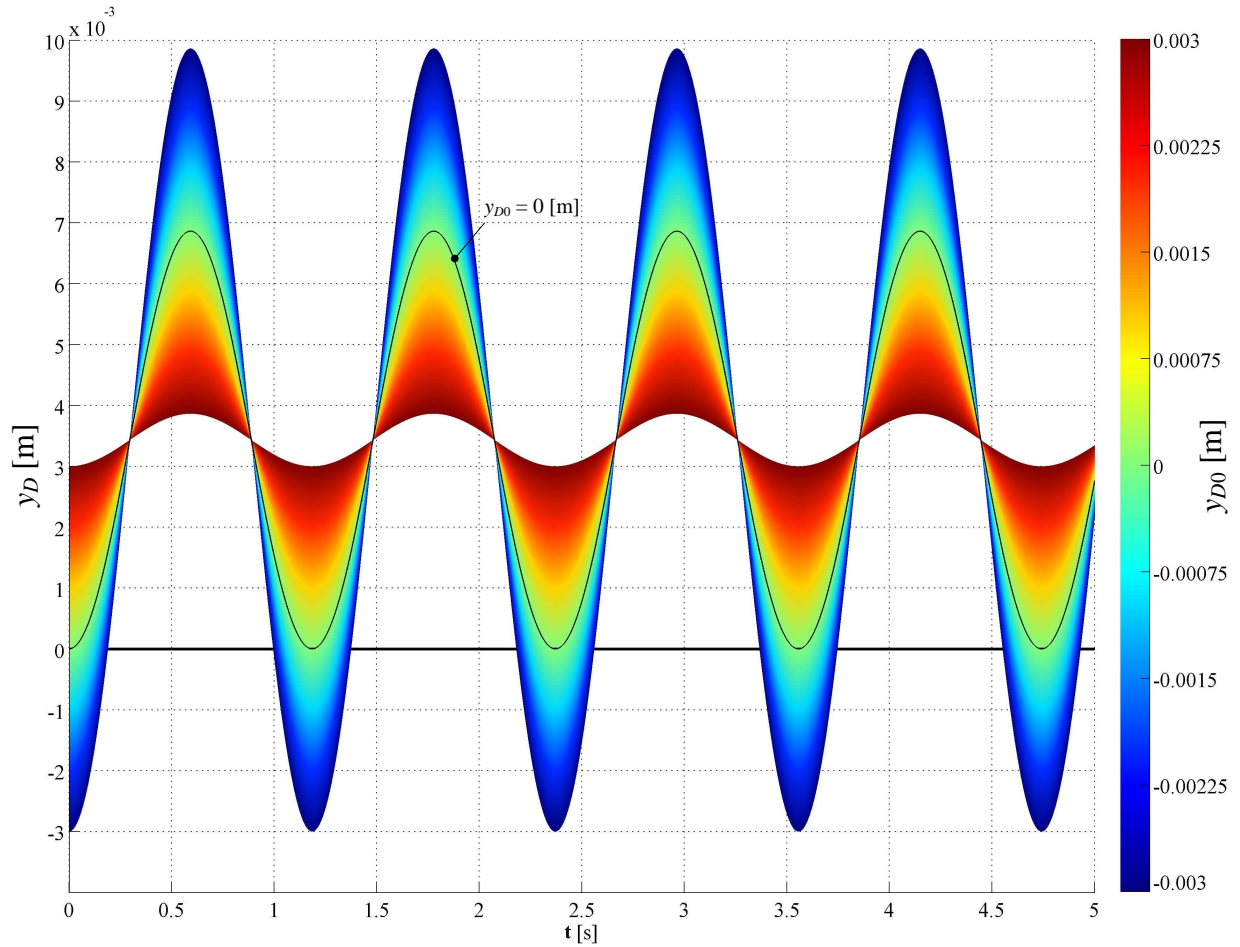


Fig. 7 Dependence $y_D = y_D(t, y_{D0})$ for $R = 2000$ m

On the basis of obtained results can be sad that lateral harmonic motion of the nonmaterial wheel set is caused by wheel conicity. The increasing of wheel conicity decreases the wave length of the harmonic motion.

3. Simulation of dynamic motion of wheel set on curved railway

3.1. Kinematic relations

For the determination of the force effect, Eq. (1), it is necessary firstly to define kinematic relations at contact points between wheel and railway. Subsequently creepage coefficients are determined for the curved railway. Wheel velocities at contact points are the same for the curved railway as for the straight railway (Švígler & Vimmr, 2006), but rail velocities, that are used by change of motions of wheel and rail, are different, Fig. 8. Virtual velocities of left and right wheels are given with expressions

$${}^L v_{11} = v \left(1 + \frac{l_0}{R} \right), \quad {}^R v_{11} = v \left(1 - \frac{l_0}{R} \right), \quad (12)$$

where $v = r_w \omega$ is the peripheral velocity of wheels in their pitch planes.

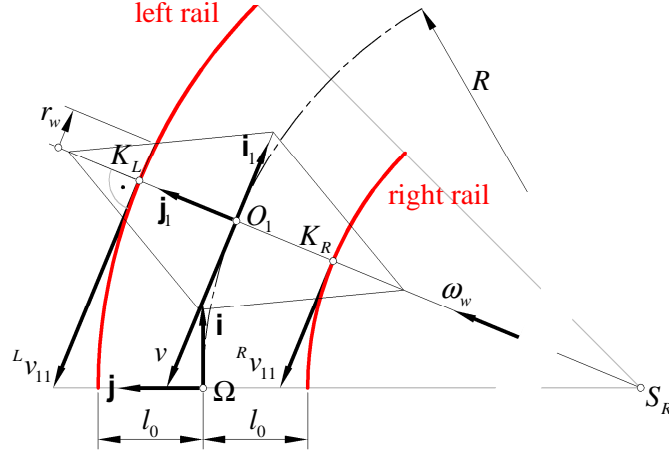


Fig. 8 Longitudinal velocities at curved railway

Using relations for creepage coefficients for the longitudinal (γ_1), lateral (γ_2) and spin (γ_3) motions (Švígler & Vimmr, 2006) in case of wheel set moving on the straight railway it is possible creepage coefficients for curved railway to express as follows

$$\begin{aligned}
 {}^L\gamma_1 &= \frac{R(r_L v + \dot{\psi} l_0 r_w)}{r_w v (R + l_0)} - 1, & {}^R\gamma_1 &= \frac{R(r_R v - \dot{\psi} l_0 r_w)}{r_w v (R - l_0)} - 1, \\
 {}^L\gamma_2 &= \frac{1}{v \left(1 + \frac{l_0}{R}\right)} \left(\dot{y} - v \frac{r_L}{r_w} \psi - l_0 \dot{\psi} \psi \right), & {}^R\gamma_2 &= \frac{1}{v \left(1 - \frac{l_0}{R}\right)} \left(\dot{y} - v \frac{r_R}{r_w} \psi + l_0 \dot{\psi} \psi \right), \\
 {}^L\gamma_3 &= \frac{1}{v \left(1 + \frac{l_0}{R}\right)} \left(\frac{v}{r_w} \lambda_L + \dot{\psi} \right), & {}^R\gamma_3 &= \frac{1}{v \left(1 - \frac{l_0}{R}\right)} \left(\frac{v}{r_w} \lambda_R + \dot{\psi} \right),
 \end{aligned} \tag{13}$$

where index L or R indicates left or right wheel.

3.2. Dynamic motion

Dynamic motion is considered as motion with two degrees of freedom which is described with equations

$$m \ddot{y}_D - m \frac{v^2}{R} - {}^L T_y - {}^R T_y + \frac{2N\lambda}{l_0} y_D = 0, \tag{14}$$

$$I_z \ddot{\psi} - (-{}^L T_y + {}^R T_y) l_0 \psi - (-{}^L T_x + {}^R T_x) l_0 - {}^L M_z - {}^R M_z = 0. \tag{15}$$

First of this equations contains centrifugal force mv^2/R and gravitational stiffness force $2N\lambda/l_0$ (Iwnicki, 2003) which is caused by total vertical load acting on wheel set.

3.3. Numerical solution

Using transformation of two second-order differential equations (14) and (15) into four first-order differential equations the numerical model in software MATLAB, that enables to simulate and to analyse motion of wheel set over railway, was created. Numerical solution was made for following entry parameters:

$v = 50$ [km/h], $R = 300$ [m], $\lambda = \arctan(1/20) \doteq 2,86^\circ$, $R_1 = \infty$ [m], $R_1' = 0,3$ [m], $r_w = 0,4575$ [m], $r_w' = 100$ [m], $l_0 = 0,750$ [m], $\sigma_1 = \sigma_2 = 0,25$ [-], $E_1 = E_2 = 2,1 \cdot 10^{11}$ [Pa], $m = 1022$ [kg], $I_z = 678$ [kg m²], $f = 0,2$ [-], $N = 20000$ [N],

where R_1 is radius of curvature of rail in longitudinal section, R_1' is radius of curvature of rail in cross section and r_w is radius of curvature of wheel in longitudinal section.

As initial values were used:

$$y_{D0} = 0,003 \text{ [m]}, \dot{y}_{D0} = 0 \text{ [ms}^{-1}\text{]}, \psi_0 = 0 \text{ [rad]}, \dot{\psi}_0 = \dot{\psi}(0) \left[\frac{\text{rad}}{\text{s}} \right].$$

Obtained results of the wheel set lateral motion on the curved railway are demonstrated in Fig. 9 – 13.

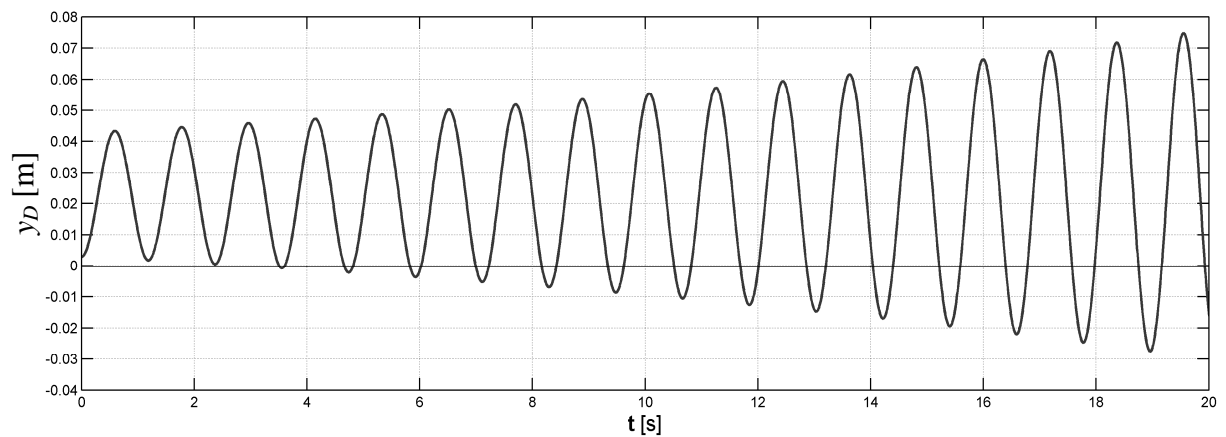


Fig. 9 Lateral motion of wheel set on curved railway

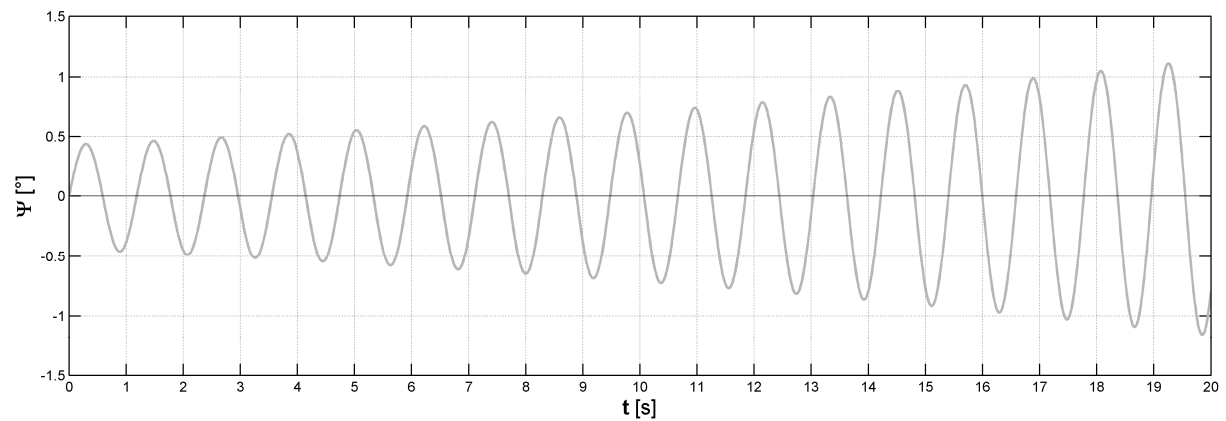


Fig. 10 Rotary motion angle ψ of wheel set on curved railway

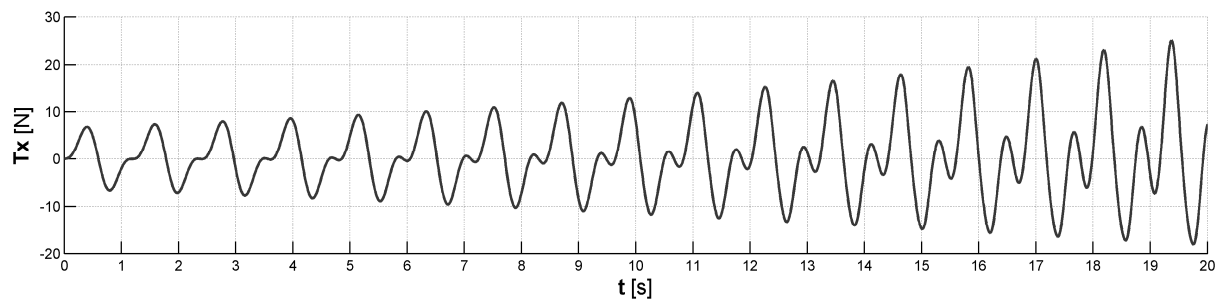


Fig. 11 Longitudinal creep force of wheel set on curved railway

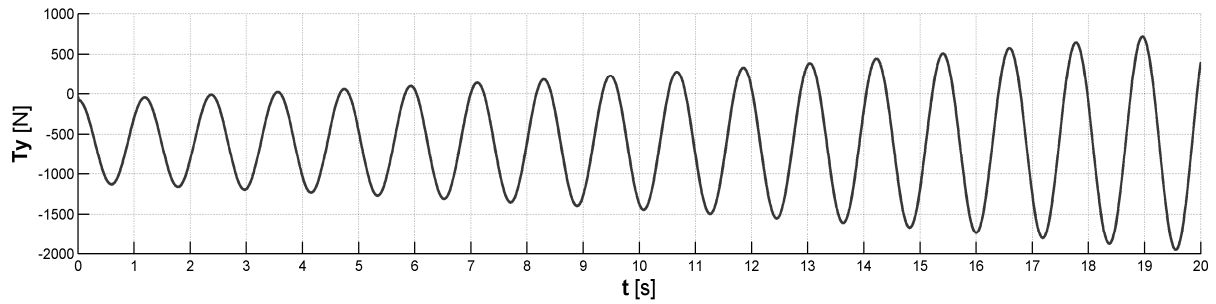


Fig. 12 Lateral creep force of wheel set on curved railway

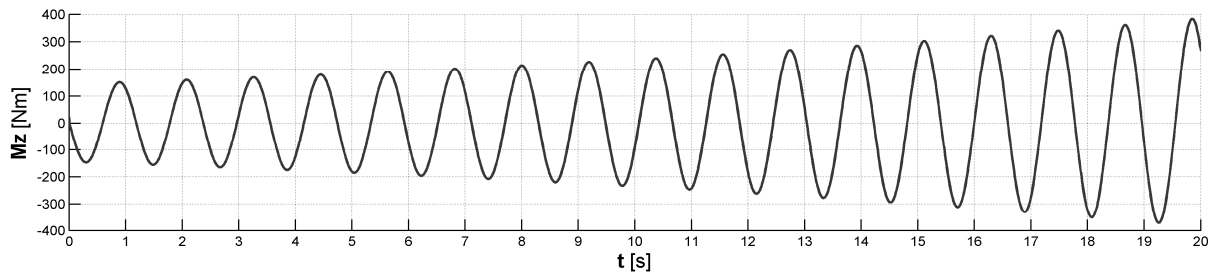


Fig. 13 Spin creep moment of wheel set on curved railway

4. Conclusion

The elementary kinematic analysis of the rolling contact between the wheel of railway vehicles and the curved railway and consequently the determination of creep forces at contact points was made. On the basis of kinematic analysis the harmonic motion of the nonmaterial wheel set on curved railway was solved. With use of determined creep forces and spin moment the motion of the material rigid wheel set on curved railway was analysed. Both motions, kinematics and dynamics, was solved numerically for the same entry parameters. Dynamics motion of the material wheel set is for velocity 50 km/h in unsteady state. Submitted paper links to analyse of motion of the wheel set on the straight railway. Obtained results create base for the appropriate analysis of motion of couple of wheel set that create a bogie of railway vehicle.

5. Acknowledgements

This work was supported by the project MŠMT 1M0519 – Research Centre of Rail Vehicles.

6. References

- De Pater, A. D. (1962) On the reciprocal pressure between two bodies. *Proceedings of symposium Rolling Contact*, pp. 29 – 75. Elsevier, Amsterdam.
- Garg, V. K. & Dukkipati, R. V. (1984) *Dynamics of Railway Vehicle Systems*. Academic publisher, London.

- Iwnicki, S. D. (2003) Simulation of wheel – rail contact forces. *Fatigue Fract Engng Mater Struct* 26, pp. 887 – 900, Blackwell Publishing Ltd., Manchester.
- Kalker, J. J. (1979) Survey of Wheel-Rail Rolling Contact Theory. *Vehicle System Dynamics* 5.
- Kalker, J. J. (1979) The computation of three dimensional rolling contact with dry friction. *International Journal for Numerical Methods Engineering* 14, pp. 1293 – 1307.
- Siegl, J. & Švígler, J. (2006) Vliv zpřesněného výpočtu creepových silových účinků na stabilitu pohybu dvojkolí. *Computational Mechanics 2006*. Hrad Nečtiny.
- Švejnoch, V. a kolektiv (1991) *Teorie kolejových vozidel*. Ediční středisko ČVUT, Prague.
- Švígler, J. & Vimmr, J. (2006) Contribution to modelling of wheel-rail contact. *Proceedings of conference Inženýrská mechanika 2006*, Svratka.